J. Fluid Mech. (1992), *vol.* 241, *pp.* 311–332
Printed in Great Britain

Water waves in shallow channels of rapidly varying depth

By A. NACHBIN† AND G. C. PAPANICOLAOU
Courant Institute of Mathematical Sciences, New York University, 251 Mercer Street, New York, NY 10012, USA

(Received 7 August 1990 and in revised form 8 October 1991)

We analyse the linear water-wave equations for shallow channels with arbitrary rapidly varying bottoms. We develop a theory for reflected waves based on an asymptotic analysis for stochastic differential equations when both the horizontal and vertical scales of the bottom variations are comparable to the depth but small compared to a typical wavelength so the shallow water equations cannot be used. We use the full, linear potential theory and study the reflection–transmission problem for time-harmonic (monochromatic) and pulse-shaped disturbances. For the monochromatic waves we give a formula for the expected value of the transmission coefficient which depends on depth and on the spectral density of the $O(1)$ random depth perturbations. For the pulse problem we give an explicit formula for the correlation function of the reflection process. We compare our theory with numerical results produced using the boundary-element method. We consider several realizations of the bottom profile, let a Gaussian-shaped disturbance propagate over each topography sampled and record the reflected signal for each realization. Our numerical experiments produced reflected waves whose statistics are in good agreement with the theory.

1. Introduction

The propagation of surface water waves in a channel with a rough bottom is in general a very difficult problem to solve analytically. A number of authors, including Carrier (1966), Hamilton (1977), Keller (1958), Kreisel (1949) and Mei & Black (1969), have studied water-wave propagation over an irregular bottom topography. A more complete set of references is given by Mei (1983). Our main interest is in the linear shallow-water regime (e.g. tidal waves) where bottom irregularities have horizontal and vertical variations that are comparable to the depth, and therefore the shallow-water approximation is not valid (Hamilton 1977).

We study the reflection–transmission problem for long waves propagating over a rapidly varying bottom topography. We are interested in pulse propagation and, eventually, in understanding how nonlinear pulses (solitons) interact with rough bottom topographies. In this paper we consider only linear problems. In order to understand the role of each Fourier component in the statistics of the reflection process, we start by considering the time-harmonic case.

In §2 we introduce the standard linear water-wave equations and the relevant lengthscales for our asymptotic analysis. In §3 we use a conformal map of the channel, as Hamilton (1977) did, in order to write (in §4) a modal decomposition for

† Present address: Department of Mathematics, The Ohio State University, 231 W 18th Avenue, Columbus, OH 43210–1174, USA.

the monochromatic wave potential. Still in §4, we derive a set of stochastic differential equations for the amplitudes of the propagating and evanescent modes, that lead to a Ricatti equation that can be analysed by asymptotic methods, as in Kohler & Papanicolaou (1973, 1974) and Papanicolaou (1978) for time harmonic waves and their extension to pulses (Asch *et al.* 1991; Burridge *et al.* 1989). In §5 we formulate the reflection problem for the time harmonic case. We present the results from the asymptotic analysis of the relevant stochastic differential equations in §6. The main result is that although the shallow-water equations are not valid for rapidly varying bottoms, the statistical properties of the reflected waves are qualitatively the same as if the stochastic analysis were performed directly on the shallow-water equations. We give an expression for the expected value of the transmission coefficient showing the localization of long waves (i.e. the transmission coefficient decays exponentially with the length of the rough region) and containing depth effects.

In §7 we use the results of the time harmonic case to extend our analysis to pulse-shaped disturbances by using the theory developed for acoustic waves (Asch *et al.* 1991; Burridge *et al.* 1989). We give an expression for the reflected power which shows how its rate of decay in time depends on depth and on the statistics of the bottom irregularities.

In order to understand better the interplay between the different scales in the problem, we have developed a computer code that calculates surface wave motion numerically. With this code we performed a series of numerical experiments and computed statistical properties of the reflected waves generated by the interaction with the topographies sampled. In order to be able to compare the theoretical with the computational results, we give, in §8, an approximate way of computing the effective parameters for scattering. For the numerical experiments we use the boundary-element method, which is briefly outlined in §9. The code has been tested and calibrated carefully (Nachbin & Papanicolaou 1992) so that it can be used for wave propagation over long distances where our asymptotic theory holds. Section 10 contains several subsections explaining in detail the numerical validation of the asymptotic theory. The numerical results are in very good agreement with the theory.

2. Formulation and scaling

The velocity potential $\phi(x, y, t)$ satisfies the linear equations (Whitham 1974):

$$\phi_{xx}+\phi_{yy}=0 \quad \text{for} \quad -h_0 H(x/l_b) < y < 0,$$

with the free-surface condition

$$\phi_{tt} = -g\phi_y \quad \text{at} \quad y = 0,$$

the Neumann condition at the bottom

$$\phi_y + h_0/l_b H'(x/l_b)\,\phi_x = 0 \quad \text{along} \quad y = -h_0 H(x/l_b)$$

and the following initial conditions given at the free surface:

$$\phi(x,0,0) = Af\left(\frac{x+c_0 t}{l_p}\right)\Big|_{t=0}, \quad \phi_t(x,0,0) = \frac{Ac_0}{l_p} f'\left(\frac{x+c_0 t}{l_p}\right)\Big|_{t=0}.$$

The function f is smooth and has compact support in $[0, \infty)$. The constant A has

dimensions of length squared over time so that f is dimensionless. The bottom topography is described by the continuous function $y = h_0 H(x/l_b)$, where

$$H(x/l_b) = \begin{cases} 1+n(x/l_b) & \text{when } -L < x < 0, \\ 1 & \text{when } x \leqslant -L \quad \text{or } x \geqslant 0. \end{cases}$$

We have introduced the lengthscales l_p (pulse width), h_0 (depth), l_b (horizontal lengthscale for bottom irregularities) and L (total length of the rough region). The acceleration due to gravity is denoted by g and the reference shallow-water speed is $c_0 = (gh_0)^{\frac{1}{2}}$. The bottom profile is a rapidly varying, zero mean, random process $n(x/l_b)$ about the undisturbed depth $y = -h_0$ and such that $|n| < 1$. We assume that there are no deterministic discontinuities in the mean depth which is h_0 throughout the channel and that the random fluctuations have rapidly decaying correlations, as in Papanicolaou & Kohler (1975). Note also that we need not assume that the fluctuations, n, are small.

We now adopt the dimensionless variables

$$x' = x/l_b, \quad y' = y/h_0, \quad t' = (c_0/l_b)\,t,$$

and define some ratios of lengthscales which identify the regime of interest in wave reflection when ordered by a small parameter $\epsilon > 0$:

$h_0/l_b = O(1) = \gamma_h$ (bottom irregularities are comparable to the depth),

$l_p/l_b = \gamma_p/\epsilon$ (incident pulse is broad compared to the bottom irregularities),

$L/l_b = \gamma_L/\epsilon^2$ (pulse penetrates in a long, rough channel).

The parameters γ_h, γ_p and γ_L are of order one and are related to the microscopic, intermediate and macroscopic scales respectively. This scaling was introduced in Burridge *et al.* (1989) where the incident pulse is meant to be a probe: the pulse width is broad compared to the scale of the irregularities so it will not feel them in detail, but narrow compared to the macroscopic scale (channel length) so that it can resolve slow variations in the topography. In this paper, we have taken a uniform mean bottom topography in order to simplify the analysis and focus on effects due to the rapid depth variations of the channel.

Consider as the dimensionless potential $\phi' = \phi/[A(\epsilon\gamma_p)^{\frac{1}{2}}]$. We introduce the square-root term so that the energy of the pulse (in the macroscopic scale, cf. equations (50)–(52)) is independent of the dimensionless parameters. We rewrite the problem in dimensionless quantities (and we drop the primes):

$$\gamma_h^2 \phi_{xx} + \phi_{yy} = 0 \quad \text{for } -H(x) < y < 0, \tag{1}$$

with the free-surface condition

$$\phi_{tt} = -1/\gamma_h^2 \phi_y \quad \text{at } y = 0, \tag{2}$$

the condition at the bottom

$$\phi_y + \gamma_h^2 H'(x)\,\phi_x = 0 \quad \text{along } y = -H(x) \tag{3}$$

and the following initial conditions given at the free surface:

$$\left.\begin{aligned} \phi(x,0,0) &= \frac{1}{(\epsilon\gamma_p)^{\frac{1}{2}}} f\left(\epsilon\frac{x+t}{\gamma_p}\right)\Big|_{t=0}, \\ \phi_t(x,0,0) &= \frac{\epsilon^{\frac{1}{2}}}{(\gamma_p)^{\frac{3}{2}}} f'\left(\epsilon\frac{x+t}{\gamma_p}\right)\Big|_{t=0}. \end{aligned}\right\} \tag{4}$$

The bottom profile is given by:

$$H(x) = \begin{cases} 1+n(x) & \text{when } -\gamma_{\mathrm{L}}/\epsilon^2 < x < 0 \\ 1 & \text{when } x \leqslant -\gamma_{\mathrm{L}}/\epsilon^2 \quad \text{or } x \geqslant 0. \end{cases} \tag{5}$$

We will study the reflection–transmission problem for equations (1)–(5) when the parameter ϵ is small.

In order to stay close to the theory developed previously, we will assume that the pulse shape function f in (4) is Gaussian-like. The initial surface elevation, obtained from $\eta(x,t) = -\phi_t(x,0,t)$, is then an **N**-shaped pulse, which is unusual for a water-wave problem. The typical case is when the initial surface elevation is Gaussian-like and then the initial velocity potential is **S**-shaped. The analysis we give here extends to this case, as we explain at the end of §7.

3. Conformal mapping

The analysis of (1)–(5) when ϵ is small is most convenient when the irregular bottom topography is transformed by a change of variables to a flat one. In the new orthogonal curvilinear variables (ξ,ζ) the equations have the form:

$$\phi_{\xi\xi}+\phi_{\zeta\zeta} = 0 \quad (-\gamma_{\mathrm{h}} < \zeta < 0) \tag{6}$$

with the free-surface condition

$$-(1+m(\xi))\,\phi_{tt} = 1/\gamma_{\mathrm{h}}\,\phi_{\zeta} \quad \text{at } \zeta = 0, \tag{7}$$

the Neumann condition at the bottom

$$\phi_{\zeta} = 0 \quad \text{at } \zeta = -\gamma_{\mathrm{h}}, \tag{8}$$

and the initial conditions

$$\phi(\xi,0,0) = \frac{1}{(\epsilon\gamma_{\mathrm{p}})^{\frac{1}{2}}} f\left(\frac{\xi+t}{\gamma_{\mathrm{p}}}\right)\Big|_{t=0}, \tag{9}$$

$$\phi_t(\xi,0,0) = \frac{\epsilon^{\frac{1}{2}}}{(\gamma_{\mathrm{p}})^{\frac{3}{2}}} f'\left(\epsilon\frac{\xi+t}{\gamma_{\mathrm{p}}}\right)\Big|_{t=0}, \tag{10}$$

given at the free surface. The new coefficient $m(\xi)$ in the free-surface condition is related to the bottom irregularities. The equations given in this form suit better the modal decomposition presented in the next section.

Following Hamilton (1977) we now describe the conformal mapping from (x,y) to (ξ,ζ). Figure 1 gives a schematic representation of the two-coordinate systems. We define a symmetric flow domain by reflecting the original one about the free surface. We denote this domain by Ω_z where $z = x+\mathrm{i}\gamma_{\mathrm{h}}\,y$ and consider it as the conformal image of the domain Ω_w where $w = \zeta+\mathrm{i}\zeta$ with $|\zeta| \leqslant \gamma_{\mathrm{h}}$. Then

$$z = x(\xi,\zeta)+\mathrm{i}\gamma_{\mathrm{h}}\,y(\xi,\zeta) = x(\xi,\zeta)+\mathrm{i}\tilde{y}(\xi,\zeta)$$

with x and $\tilde{y}$ a pair of harmonic functions on Ω_w. The imaginary part of the conformal map is a harmonic function that is defined by

$$\Delta\tilde{y}(\xi,\zeta) = 0 \quad \text{in } \Omega_w, \tag{11}$$

with Dirichlet boundary conditions

$$\tilde{y}(\xi,\pm\gamma_{\mathrm{h}}) = \pm\gamma_{\mathrm{h}} H(x(\xi,\pm\gamma_{\mathrm{h}})), \tag{12}$$

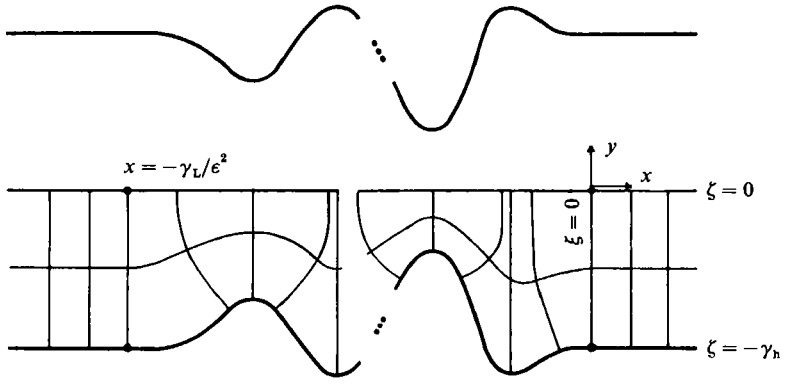

FIGURE 1. Coordinate systems xy and $\xi\zeta$ and the symmetric flow domain.

where $x(\xi, \zeta)$ is its harmonic conjugate. We have a Green's function for problem (11), (12) which is slightly different from Hamilton's because we keep depth effects through the depth parameter γ_h. The Green's function, vanishing along the lines $\zeta = \pm\gamma_h$, is given by

$$G(w; w_0) = \operatorname{Re}\log\left(\frac{\exp(\frac{1}{2}\pi w/\gamma_h) - \exp(\frac{1}{2}\pi w_0/\gamma_h)}{\exp(\frac{1}{2}\pi w/\gamma_h) + \exp(\frac{1}{2}\pi \bar{w}_0/\gamma_h)}\right), \tag{13}$$

where Re stands for the real part and the overbar denotes complex conjugation. Using Green's third identity we have

$$\tilde{y}_{\zeta_0}(\xi_0, 0) = \frac{\pi}{4\gamma_h^2}\int_{-\infty}^{\infty} \frac{\gamma_h H(x(\xi, -\gamma_h))}{\cosh^2[(\pi/2\gamma_h)(\xi - \xi_0)]} d\xi. \tag{14}$$

In the (ξ, ζ)-coordinate system the rapidly varying bottom topography has been straightened out but now the coefficient in the surface boundary condition is rapidly varying, although in a slightly smoother way because of the depth effects. To express this coefficient in (ξ, ζ)-coordinates note first that

$$\int_{-\infty}^{\infty} \frac{\pi}{4\gamma_h} \operatorname{sech}^2\left[\frac{\pi}{2\gamma_h}(x-y)\right] dx = \tfrac{1}{2}\tanh\left[\frac{\pi}{2\gamma_h}x\right]_{-\infty}^{\infty} = 1.$$

Hence as $\gamma_h \downarrow 0$ the kernel goes to a delta function and the original perturbations of the bottom are felt at the free surface level without any smoothing. Another way of saying this is that when $\gamma_h \downarrow 0$ the bottom variations are on a sufficiently long scale, compared to the depth scale, so that the coordinate transformation is not necessary. Using the definition of the bottom profile $H(x)$ we may write $\tilde{y}_{\zeta_0}(\xi_0, 0) = 1 + m(\xi_0)$ with

$$m(\xi_0) \equiv \frac{\pi}{4\gamma_h}\int_{-\infty}^{\infty} \frac{n(x(\xi, -\gamma_h))}{\cosh^2[(\pi/2\gamma_h)(\xi - \xi_0)]} d\xi = [K*(n \circ x)](\xi_0). \tag{15}$$

Regarding the initial conditions (given in the transformed coordinate system) we note that by starting with the pulse located over a region of uniform depth, the initial data are affected very little by the mapping as ϵ tends to zero. We can replace x by ξ, noting that away from the rough region $y_\xi(\xi, 0) \approx 1$ (how far depends on γ_h) and therefore from the Cauchy–Riemann equation $x_\xi(\xi, 0) \approx 1$. We can then take the interval $[x = -\gamma_L/\epsilon^2, x = 0]$ occupied by the rough channel as the image of $[\xi = -\gamma_L^\xi/\epsilon^2, \xi = 0]$. Up to a correction of order ϵ^2, γ_L^ξ is equal γ_L.

4. Modal decomposition for the time harmonic problem

Having transformed the problem to one with a flat bottom topography but with a variable coefficient in the free surface condition, we can now decompose the potential into a superposition of wave modes. The interplay between these modes is better understood if we initially consider time harmonic waves (i.e. monochromatic waves of frequency ω). We will see in the next section that only propagating modes contribute in the stochastic problem. We then extend our results to the original pulse problem.

We now introduce the modal expansion. For simplicity we will change notation so that by x and y we mean the orthogonal curvilinear pair (ξ, ζ). Consider the time harmonic case in which waves of a given frequency ω are studied. Assume that the potential is the form

$$\Phi(x, y, t) = \mathrm{e}^{-\mathrm{i}\omega t}\phi(x, y).$$

The reduced potential $\phi(x, y)$ must satisfy

$$\phi_{xx} + \phi_{yy} = 0 \quad (-\gamma_\mathrm{h} < y < 0), \tag{16}$$

with

$$\omega^2(1 + m(x))\phi = 1/\gamma_\mathrm{h}\phi_y \quad \text{at } y = 0, \tag{17}$$

and

$$\phi_y = 0 \quad \text{at } y = -\gamma_\mathrm{h}. \tag{18}$$

A *propagating mode* of the unperturbed problem, where $m \equiv 0$, is a solution of the form

$$\phi_0(x, y) = \mathrm{e}^{\pm \mathrm{i}k_0 x}\psi_0(y), \quad \psi_0(y) = \cosh(k_0(\gamma_\mathrm{h} + y)), \tag{19}$$

where k_0 satisfies the dispersion relation

$$\omega^2 = k_0/\gamma_\mathrm{h}\tanh(k_0\gamma_\mathrm{h}). \tag{20}$$

An *evanescent mode* has the form

$$\phi_j(x, y) = \exp(\pm k_j x)\psi_j(y), \quad \psi_j(y) = \cos[k_j(\gamma_\mathrm{h} + y)], \tag{21}$$

where

$$\omega^2 = -k_j/\gamma_\mathrm{h}\tan(k_j\gamma_\mathrm{h}) \quad (j = 1, 2, \ldots). \tag{22}$$

The reduced eigenfunctions $\psi_j(y)$ $(j = 0, 1, \ldots)$ form an orthogonal set (Kreisel 1949; Nachbin 1989).

We now express the solution to the perturbed time harmonic problem in

$$-\gamma_\mathrm{L}/\epsilon^2 < x < 0$$

as a superposition of the unperturbed modes with variable amplitudes:

$$\phi(x, y) = A_0(x)\cosh(k_0(\gamma_\mathrm{h} + y))\exp(\mathrm{i}k_0 x) + B_0(x)\cosh(k_0(\gamma_\mathrm{h} + y))\exp(-\mathrm{i}k_0 x)$$
$$+ \sum_{j=1}^{\infty}\{A_j(x)\cos[k_j(\gamma_\mathrm{h} + y)]\exp[k_j(x + \gamma_\mathrm{L}/\epsilon^2)] + B_j(x)\cos[k_j(\gamma_\mathrm{h} + y)]\exp(k_j x)\}. \tag{23}$$

The amplitudes $A_0(x)$, $B_0(x)$, $A_j(x)$ and $B_j(x)$ are stochastic processes whose statistical properties we wish to determine. As in the variation of constants method in ordinary differential equations we may impose the additional condition

$$[A_0'(x)\exp(\mathrm{i}k_0 x) + B_0'(x)\exp(-\mathrm{i}k_0 x)]\psi_0$$
$$+ \sum_{j=1}^{\infty}\left\{A_j'(x)\exp\left[-k_j\left(x + \frac{\gamma_\mathrm{L}}{\epsilon^2}\right)\right] + B_j'(x)\exp(k_j x)\right\}\psi_j = 0. \tag{24}$$

From the equations for ϕ we get equations for the mode amplitudes. Multiplying (16)

by ψ_j, integrating over y from $-\gamma_h$ to 0 and integrating by parts in the y variable we have

$$\frac{d^2}{dx^2}\int_{-\gamma_h}^{0}\psi_j\phi\,dy+\int_{-\gamma_h}^{0}\psi_j''\phi\,dy=-[\psi_j\phi_y-\psi_j'\phi]_{-\gamma_h}^{0},$$

which represents an infinite system of first-order differential equations when we use (23) and (24). We complete our infinite set of differential equations by also projecting condition (24). Redefining the amplitudes of the evanescent modes as

$$A_j\equiv A_j\exp[-k_j(x+\gamma_L/\epsilon^2)]$$

and $B_j\equiv B_j\exp(k_jx)$ we obtain the system

$$A_0'(x)=\frac{i}{2k_0}\frac{\omega^2m(x)(\psi_0\phi)_{y=0}}{\|\psi_0\|^2}\exp(-ik_0x), \tag{25}$$

$$B_0'(x)=-\frac{i}{2k_0}\frac{\omega^2m(x)(\psi_0\phi)_{y=0}}{\|\psi_0\|^2}\exp(ik_0x), \tag{26}$$

and for $j\geqslant 1$

$$A_j'(x)=-k_jA_j(x)+\frac{1}{2k_j}\frac{\omega^2m(x)(\psi_j\phi)_{y=0}}{\|\psi_j\|^2}, \tag{27}$$

$$B_j'(x)=k_jB_j(x)-\frac{1}{2k_j}\frac{\omega^2m(x)(\psi_j\phi)_{y=0}}{\|\psi_j\|^2}, \tag{28}$$

where $(\psi_j\phi)_{y=0}$ indicates evaluation along the free surface. Note that ϕ is given by (23) evaluated at $y=0$.

By writing the water-wave equations in the orthogonal curvilinear coordinates we have derived an infinite system of stochastic differential equations for the amplitudes A_0 and B_0 of the propagating modes and the amplitudes A_j and B_j of the evanescent modes. We are now in a position to formulate the reflection problem. We will show that only two equations, of this infinite system, are relevant to the asymptotic analysis given in §6.

5. The reflection problem for the time-harmonic case

The main point of our asymptotic analysis is that only propagating modes contribute to the statistical reflection–transmission problem in our scaling. This is best seen in the reflection and transmission of time-harmonic wavetrains incident on a segment of channel that has a rough bottom. We will analyse this problem first, in this and the next section, and return to pulses in §7.

When a wave of unit amplitude is incident from the right the amplitude equations (25)–(28) have to be solved in $-\gamma_L/\epsilon^2\leqslant x\leqslant 0$ subject to the two-point boundary conditions

$$A_0(-\gamma_L/\epsilon^2)=0,\quad A_j(-\gamma_L/\epsilon^2)=0,\quad B_0(0)=1,\quad B_j(0)=0.$$

These boundary conditions are not exact because $m(x)$ (cf. (15)) is not identically zero (but it decays exponentially fast to zero) away from this interval and the decay rate is proportional to $(\gamma_h\epsilon^2)^{-1}$ on the macroscopic scale. This discrepancy is negligible in the asymptotic limit analysed here.

The system of equations (25)–(28) can be written in matrix form when the amplitudes are arranged into the vector

$$[A_0(x)\dots A_j(x)\dots B_0(x)\dots B_j(x)\dots]^T.$$

Then the system becomes

$$\frac{\mathrm{d}}{\mathrm{d}x}\boldsymbol{\Phi} = \begin{bmatrix} \boldsymbol{D} & 0 \\ 0 & -\boldsymbol{D} \end{bmatrix}\boldsymbol{\Phi} + \begin{bmatrix} \boldsymbol{M}_{11} & \boldsymbol{M}_{12} \\ \boldsymbol{M}_{21} & \boldsymbol{M}_{22} \end{bmatrix}\boldsymbol{\Phi}, \tag{29}$$

where $\boldsymbol{\Phi}$ denotes the fundamental solution matrix, $\boldsymbol{D}$ is the diagonal matrix $\mathrm{diag}\{0, -k_j, \ldots\}$, $j = 1, 2, \ldots$ and $\boldsymbol{M}_{ij}$ are infinite-order submatrices obtained from the right-hand side of the system. If we partition $\boldsymbol{\Phi}$ in the same way as we did for $\boldsymbol{M}$ and let $\boldsymbol{Z} \equiv \boldsymbol{\Phi}_{12}\boldsymbol{\Phi}_{22}^{-1}$ then the solution of the two-point boundary value problem is obtained from

$$[A_0(x) \ldots A_j(x) \ldots]^{\mathrm{T}} = \boldsymbol{Z}(x)\,[B_0(x) \ldots B_j(x) \ldots]^{\mathrm{T}}.$$

The reflection matrix $\boldsymbol{Z}$ satisfies the matrix Riccati equation

$$\mathrm{d}\boldsymbol{Z}/\mathrm{d}x = \boldsymbol{D}\boldsymbol{Z} + \boldsymbol{Z}\boldsymbol{D} + \boldsymbol{M}_{11}\boldsymbol{Z} + \boldsymbol{M}_{12} - \boldsymbol{Z}\boldsymbol{M}_{21}\boldsymbol{Z} - \boldsymbol{Z}\boldsymbol{M}_{22} \tag{30}$$

in $-\gamma_{\mathrm{L}}/\epsilon^2 \leqslant x \leqslant 0$ with $\boldsymbol{Z}(-\gamma_{\mathrm{L}}/\epsilon^2) = 0$.

Since $Z_{00}(0)$ is the reflection coefficient, the quantity of interest, we must now analyse the stochastic Riccati equation (30) as ϵ tends to zero. We know from basic localization-length ideas (Arnold, Papanicolaou & Wihstutz 1986 and references therein) that low frequencies will penetrate into a channel which is long. We also know that high-frequency modes are in a deep-water regime and therefore are insensitive to bottom variations. These modes penetrate into a long rough channel and generate no reflection (this is confirmed in Devillard, Dunlop & Souillard 1988). Hence we will focus on long waves and we introduce the scaled frequency $\omega \to \epsilon\omega$ and the macroscopic distance into the rough channel $x \to x/\epsilon^2$. Scaled in this way, (30) is ready for asymptotic analysis except that we must first evaluate the approximate form of $\boldsymbol{D}$ and $\boldsymbol{M}_{ij}$. We find easily that for ϵ small

$$k_0 \approx \pm\epsilon\omega\,(1 + \tfrac{1}{6}\epsilon^2\omega^2\gamma_{\mathrm{h}}^2), \tag{31}$$

and

$$k_j \approx \left(\frac{\pi j}{\gamma_{\mathrm{h}}} - \frac{\epsilon^2\omega^2\gamma_{\mathrm{h}}}{\pi j}\right) \quad (j = 1, 2, \ldots), \tag{32}$$

while the coupling matrices become

$$\boldsymbol{M}_{11} \approx \mathrm{i}\alpha^{\epsilon}\begin{bmatrix} 1 \ldots (-1)^j\beta^{-1} \\ 0 \ldots \quad 0 \\ 0 \ldots \quad 0 \end{bmatrix}, \quad \boldsymbol{M}_{12} \approx \mathrm{i}\alpha^{\epsilon}\begin{bmatrix} \beta^{-2} \ldots (-1)^j\beta^{-1} \\ 0 \quad \ldots \quad 0 \\ 0 \quad \ldots \quad 0 \end{bmatrix} \tag{33}$$

$$\boldsymbol{M}_{21} \approx \mathrm{i}\alpha^{\epsilon}\begin{bmatrix} \beta^{-2} \ldots (-1)^j\beta \\ 0 \quad \ldots \quad 0 \\ 0 \quad \ldots \quad 0 \end{bmatrix}, \quad \boldsymbol{M}_{22} \approx -\mathrm{i}\alpha^{\epsilon}\begin{bmatrix} 1 \ldots (-1)^j\beta \\ 0 \ldots \quad 0 \\ 0 \ldots \quad 0 \end{bmatrix} \tag{34}$$

with

$$\alpha^{\epsilon}(x) \equiv \alpha(x/\epsilon^2), \quad \alpha(x) \equiv 0.5\omega m(x)/\gamma_{\mathrm{h}}, \quad \beta(x) \equiv \exp[(-\mathrm{i}\omega x)/\epsilon]. \tag{35}$$

We can now use the asymptotic analysis for stochastic equations on (30). The most directly applicable version of this theory is in Kohler (1977) but it is also described in Papanicolaou (1978), Papanicolaou & Kohler (1975) and in references cited therein as well as in Asch *et al.* (1991) and Burridge *et al.* (1989). The typical system given in Kohler (1977) and Papanicolaou & Kohler (1975) has N propagating and M decaying solutions. Using the approximations given by (31) and (32) we see that the entries of the first two matrices of the Riccati equation (30) are

$$[\boldsymbol{Z}\boldsymbol{D} + \boldsymbol{D}\boldsymbol{Z}]_{ij} \approx -\pi/\gamma_{\mathrm{h}}\,(i+j)\,Z_{ij} \quad (i, j = 0, 1, 2, \ldots),$$

and therefore the only non-decaying entry is $Z_{00}(x)$. This is a complex-valued entry of the reflection matrix, which implies $N = 2$. All the other entries are decaying and there are infinitely many of them. We could have truncated the modal expansion so that only a finite number of evanescent modes were taken into account. As we shall see, however, they play no role in the asymptotic analysis of the stochastic Riccati equation anyway.

For the non-decaying mode we have

$$\frac{\mathrm{d}}{\mathrm{d}x}Z_{00} = \frac{\mathrm{i}\alpha^{\epsilon}(x)}{\epsilon}\Bigg[2Z_{00} + \beta^{-1}(x)\sum_{j=1}^{\infty}(-1)^j Z_{j0} + \beta^{-2}(x) + Z_{00}\Bigg(Z_{00}\beta^2(x) + \beta(x)\sum_{j=1}^{\infty}(-1)^j Z_{j0}\Bigg)\Bigg] + O(1)\ \text{(mean zero term)}, \quad (36)$$

where the terms omitted are of order one relative to ϵ and have zero mean so that they do not contribute in the limit. The vector field for this equation depends only on the entries of the first column of $\boldsymbol{Z}$. These are the only entries that could couple with Z_{00} in the asymptotic analysis, as given in the second term of the drift coefficient (cf. Kohler 1977, p. 527). In the next section we will give the diffusion equation that comes from the asymptotic analysis of these equations. The elements in the first column of $\boldsymbol{Z}$ satisfy (for $j \geqslant 1$):

$$\frac{\mathrm{d}}{\mathrm{d}x}Z_{j0} = \frac{1}{\epsilon^2}\left(\frac{-\pi j}{\gamma_{\mathrm{h}}}Z_{j0}\right) + \frac{\mathrm{i}\alpha^{\epsilon}(x)}{\epsilon}\Bigg[Z_{j0} + Z_{j0}\Bigg(Z_{00}\beta^2(x) + \beta(x)\sum_{j=1}^{\infty}(-1)^j Z_{j0}\Bigg)\Bigg]. \quad (37)$$

From the formulae in Kohler (1977) (for the drift coefficient of the associated diffusion problem) we see that when the order $1/\epsilon$ right-hand side is evaluated at $Z_{j0} = 0, j \geqslant 1$, it becomes identically zero. Hence the second contribution to the drift coefficient is zero. The third contribution is also zero for it comes from averaging the order one (mean zero) term in the equation for Z_{00}. Thus, to find the associated diffusion operator we can restrict ourselves to the equation for Z_{00} alone, with all Z_{j0} in it equal to zero.

6. Asymptotic analysis of the reflection process

In the previous section we showed that the only non-decaying entry of the reflection matrix $\boldsymbol{Z}$ is Z_{00} so we restrict our study to it. We are primarily interested in the modulus of the reflection coefficient Z_{00}. By adopting a polar coordinate representation we shall characterize its asymptotic limit as ϵ tends to zero in terms of a one-dimensional diffusion process. Let

$$Z_{00} = r\mathrm{e}^{\mathrm{i}\varphi},$$

and consider the vector field in (36) already evaluated at $Z_{j0} = 0$, $j \neq 0$. From conservation of energy we know that $r \in [0, 1]$. Letting $r = \tanh(\frac{1}{2}\theta)$, with $\theta > 0$ the stochastic equation (36) becomes the simple system

$$\frac{\mathrm{d}\theta}{\mathrm{d}x} = \frac{2\alpha^{\epsilon}}{\epsilon}\sin\left(\varphi + \frac{2\omega x}{\epsilon(\gamma_{\mathrm{h}})^{\frac{1}{2}}}\right), \quad (38)$$

$$\frac{\mathrm{d}\varphi}{\mathrm{d}x} = \frac{2\alpha^{\epsilon}}{\epsilon}\left[1 + \coth\theta\cos\left(\varphi + \frac{2\omega x}{\epsilon(\gamma_{\mathrm{h}})^{\frac{1}{2}}}\right)\right], \quad (39)$$

where $\alpha^{\epsilon}(x)$ is a random process in $[-\gamma_{\mathrm{L}}, 0]$ defined by (35).

We will not go into details of how the solution of (38) and (39) converges, as ϵ tends to zero, to a diffusion process as this is done in the papers cited above. We will define directly this limiting diffusion from its infinitesimal generator, that is, from its diffusion and drift coefficients. They are calculated according to the formulae given in Kohler (1977) and this leads to the diffusion operator

$$\mathscr{L}_\theta \equiv \frac{\omega^2}{2\gamma_h^2}\alpha_{mm}\left(\frac{\partial^2}{\partial\theta^2}+\coth\theta\frac{\partial}{\partial\theta}\right), \tag{40}$$

where

$$\alpha_{mm} \equiv \int_0^\infty E\{m(s)\,m(0)\}\,\mathrm{d}s \tag{41}$$

is the integral of the correlation function, or its Fourier transform at zero frequency. It is therefore non-negative and we assume that it is positive here. It is very difficult to compute it because it is related to the bottom topography n (cf. (5)) through the conformal mapping and (15). We return to its calculation in §8. If we solve the diffusion equation

$$u_\tau = \mathscr{L}_\theta u,$$

with

$$u(\theta,0) = \tanh^2(\tfrac{1}{2}\theta)$$

then $u(0,\gamma_L)$ is equal to $E\{|Z_{00}(0)|^2\}$, as $\epsilon\to 0$ (Kohler 1977). However, in this limit $1-|Z_{00}|^2 = |T|^2$ where T is the transmission coefficient for the region $[-\gamma_L, 0]$ over the rough bottom. The solution to the diffusion equation above is given in Kohler & Papanicolaou (1973, 1974) and Papanicolaou (1978). We have the formula

$$\lim_{\epsilon\to 0} E\{|T|^2\} = \exp\left(-\frac{\gamma_L\omega^2}{8\gamma_h^2}\alpha_{mm}\right)\int_{-\infty}^{\infty}\exp\left(-t^2\frac{\gamma_L\omega^2}{2\gamma_h^2}\alpha_{mm}\right)\frac{\pi t\sinh\pi t}{\cosh^2\pi t}\,\mathrm{d}t. \tag{42}$$

Thus the theory predicts an exponential decay of the transmission coefficient with scaled distance γ_L, that is, localization of the wave energy. Note the effect of the scaled depth $\gamma_h = h_0/l_b$: deeper channels allow more transmission. Alternatively, we can say that irregularities varying on a shorter scale allow more transmission.

A theory for the localization of time-harmonic water waves is given by Devillard *et al.* (1988), while the results of experiments in a wave tank are presented in Belzons, Guazelli & Parodi (1988). They considered a bottom topography which is described by a random step function and the 'wide-spacing approximation' (i.e. the horizontal scale of the steps is large compared to its vertical lengthscale). No restriction is made on the wavelength λ. For the full, linear potential theory they estimate the localization length in both limits $\lambda\to\infty$ and $\lambda\to 0$ and conclude that it diverges exponentially in the latter. This is a fundamental difference between potential theory and the shallow-water theory (or its analogue, the acoustic wave theory given in Burridge *et al.* 1989). This is mainly due to the finite (and not infinitesimal) depth of the channel.

In our theory the topography is described by an arbitrary function for which the horizontal scale of the bottom variations and their amplitude, as well as the depth, are comparable. The fact that we restrict the range of wavelengths (by introducing the scaling $\omega\to\epsilon\omega$) has a negligible effect on the pulse reflection problem studied in the next section. We should point out that for the pulse-shaped disturbance to be considered, not only should higher Fourier components have amplitudes that are

exponentially small but also they must be in a deep-water regime. This is supported in Devillard *et al.* (1988).

7. The two-frequency problem and the statistics for pulse reflection

In the section above we studied the reflection–transmission problem for monochromatic waves. We now consider the case of pulse-shaped waves, which involves a full band of frequencies. We will extend to water waves the theory developed by Burridge *et al.* (1989) for acoustic wave pulses in random media. We will present the main results obtained from the asymptotic theory developed in Burridge *et al.* (1989) and the formulae we will use in the numerical validation of the theory.

To analyse the pulse reflection problem ((6)–(10)) we first rewrite it in the scaled macroscopic variables by letting $\xi = x/\epsilon^2$, $\zeta = y$ and $t = \tau/\epsilon^2$:

$$\epsilon^4 \phi_{xx} + \phi_{yy} = 0 \quad (-\gamma_h < y < 0), \tag{43}$$

with
$$-\epsilon^4 [1 + m(x/\epsilon^2)]\, \phi_{\tau\tau} = 1/\gamma_h \phi_y \quad \text{at } y = 0, \tag{44}$$

and
$$\phi_y = 0 \quad \text{at } y = -\gamma_h. \tag{45}$$

The initial conditions are:

$$\phi(x, 0, 0) = \frac{1}{(\epsilon\gamma_p)^{\frac{1}{2}}} f\left(\epsilon \frac{x+\tau}{\gamma_p}\right)\Big|_{t=0}, \tag{46}$$

$$\phi_\tau(x, 0, 0) = \frac{\epsilon^{\frac{1}{2}}}{(\gamma_p)^{\frac{3}{2}}} f'\left(\epsilon \frac{x+\tau}{\gamma_p}\right)\Big|_{t=0}. \tag{47}$$

We now show how the results of the previous section can be used to make the connection between the water-wave pulse problem and the acoustic pulse problem. When the bottom is flat (i.e. $m(x/\epsilon^2) \equiv 0$) we can superimpose the propagating modes and write for the left-going wave

$$\phi(x, y, \tau) = \int_{-\infty}^{\infty} \hat{\Phi}(\omega) \cosh[k_0(\gamma_h + y)] \exp(-i(k_0 x + \omega\tau)/\epsilon^2)\, d\omega. \tag{48}$$

As in the previous section we consider low frequencies and we put the corresponding approximation for the wavenumber k_0 in the expression above to get

$$\phi(x, y, \tau) \approx \int_{-\infty}^{\infty} \hat{\Phi}(\omega) \exp[-i\omega(x+\tau)/\epsilon]\, d\omega \equiv \Phi\left(\frac{x+\tau}{\epsilon}\right). \tag{49}$$

We can do the same type of approximation for the right-going wave. Clearly this function Φ satisfies the equation

$$\Phi_{\tau\tau} - \Phi_{xx} = 0,$$

$$\Phi(x, 0) = \frac{1}{\epsilon^{\frac{1}{2}}} f\left(\frac{x+\tau}{\epsilon}\right)\Big|_{\tau=0},$$

$$\Phi_\tau(x, 0) = \frac{1}{\epsilon^{\frac{3}{2}}} f'\left(\frac{x+\tau}{\epsilon}\right)\Big|_{\tau=0}.$$

In the time-harmonic case we saw that the evanescent modes played no role in the

asymptotic limit of the inhomogeneous case. We will therefore make the shallow-water approximation of (43)–(47) right at the beginning by dropping the evanescent modes and by considering the pulse reflection problem below:

$$[1+m(\gamma_p x/\epsilon^2)]\,\Phi_{\tau\tau}-\Phi_{xx}=0, \tag{50}$$

$$\Phi(x,0)=\frac{1}{\epsilon^{\frac{1}{2}}}f\left(\frac{x+\tau}{\epsilon}\right)\Big|_{\tau=0}, \tag{51}$$

$$\Phi_\tau(x,0)=\frac{1}{\epsilon^{\frac{3}{2}}}f'\left(\frac{x+\tau}{\epsilon}\right)\Big|_{\tau=0}. \tag{52}$$

We have adjusted the scales so that pulses are considered to be of width ϵ (in the macroscale). We must now consider the effective correlation length of the stochastic process $m(x)$, owing to the presence of the parameter γ_p in its argument.

We must clarify in what sense solutions of (43)–(47) and of (50)–(52) are close. The statistical properties of the solutions of (50)–(52), for example the mean and the mean square of Φ outside the rough region, are close to those of the original problem (43)–(47) when ϵ is small. We have demonstrated this with the theory of the single frequency reflection and transmission and we have conducted extensive numerical simulations (see §10.4) that support this approximation.

To analyse equations (50)–(52) we use the theory developed by Burridge *et al.* (1989) for acoustic wave pulses in random media. The equations for acoustic waves are

$$\rho(x)\,u_t(x,t)+p_x(x,t)=0,$$

$$\frac{1}{K(x)}p_t(x,t)+u_x(x,t)=0,$$

where $u(x,t)$ is the velocity, $p(x,t)$ is the pressure, $\rho(x)$ is the density and $K(x)$ is the bulk modulus, which in the present analogy is taken to be identically equal to one. We eliminate the pressure so that

$$-\rho(x)\,u_{tt}(x,t)+u_{xx}(x,t)+0, \tag{53}$$

$$u(x,0)=\frac{1}{\epsilon^{\frac{1}{2}}}f\left(\frac{x+t}{\epsilon}\right)\Big|_{t=0}, \tag{54}$$

$$u_t(x,0)=\frac{1}{\epsilon^{\frac{3}{2}}}f'\left(\frac{x+t}{\epsilon}\right)\Big|_{\tau=0}. \tag{55}$$

This problem is equivalent to (50)–(52).

We present the main results obtained from the asymptotic theory developed in Burridge *et al.* (1989) and the formulae we use in the numerical validation of the theory. For the analysis of this problem we Fourier transform in time, choosing a frequency scale appropriate for the pulse $f(t)$:

$$\hat{f}(\omega)=\int_{-\infty}^{\infty}e^{i\omega t}f(t)\,dt \quad \text{where } t=\tau/\epsilon.$$

We will determine the statistics of the reflected potential by studying

$$R^{\epsilon}_{t,f}(\sigma)=\frac{1}{2\pi\epsilon^{\frac{1}{2}}}\int_{-\infty}^{\infty}\exp\left[\frac{-i\omega(t+\epsilon\sigma)}{\epsilon}\right]\hat{f}(\omega)\,Z_{00}(\omega)\,d\omega. \tag{56}$$

By $Z_{00}(\omega)$ we mean the reflection coefficient (at $x = 0$) corresponding to an input of frequency ω and amplitude $\hat{f}(\omega)$. We consider the above expression as a stochastic process in σ, with t held fixed. That is, for each t we consider a 'time window' centred at t, and of duration on the order of the pulse width, with the parameter σ measuring time within this window. Statistical properties of the reflected signal over windows with different centres become independent in the limit $\epsilon \to 0$.

We will calculate the power spectrum of the window reflection process $R^{\epsilon}_{t,f}(\sigma)$ as $\epsilon \to 0$. Consider the correlation function

$$C^{\epsilon}_{t,f}(\sigma) \equiv E\{R^{\epsilon}_{t,f}(\sigma)\, R^{\epsilon}_{t,f}(0)\} = \frac{1}{4\pi^2\epsilon}\int_{-\infty}^{\infty} \mathrm{d}\omega_1 \int_{-\infty}^{\infty} \mathrm{d}\omega_2 \exp\left(\frac{-\mathrm{i}\omega_1 t}{\epsilon}\right)\exp(-\mathrm{i}\omega_1\sigma)$$
$$\times \exp\left(\frac{\mathrm{i}\omega_2 t}{\epsilon}\right)\hat{f}(\omega_1)\,\bar{\hat{f}}(\omega_2)\, E\{Z_{00}(\omega_1)\,\bar{Z}_{00}(\omega_2)\}. \tag{57}$$

Changing variables ($\omega_1 = \omega - \frac{1}{2}\epsilon h$ and $\omega_2 = \omega + \frac{1}{2}\epsilon h$) we define

$$u^{\epsilon}(\omega, h) \equiv E\{Z_{00}(\omega - \tfrac{1}{2}\epsilon h)\,\bar{Z}_{00}(\omega + \tfrac{1}{2}\epsilon h)\}. \tag{58}$$

Then $C^{\epsilon}_{t,f}(\sigma)$ is such that

$$\lim_{\epsilon \downarrow 0} C^{\epsilon}_{t,f}(\sigma) = \frac{1}{2\pi}\int_{-\infty}^{\infty} \mathrm{d}\omega \exp(-\mathrm{i}\omega\sigma)|\hat{f}(\omega)|^2 \frac{1}{2\pi}\int_{-\infty}^{\infty} \mathrm{d}h\, \mathrm{e}^{\mathrm{i}ht} \lim_{\epsilon \downarrow 0} u^{\epsilon}(\omega, h). \tag{59}$$

The problem reduces to studying the joint statistics of two neighbouring frequencies (cf. (58)) in the limit as ϵ goes to zero, if we ignore the difficulty in interchanging this limit with integration which requires more analysis. The limit

$$u(\omega, h) = \lim_{\epsilon \downarrow 0} u^{\epsilon}(\omega, h)$$

exists, and its transform is given by

$$\mu(t, \omega) = \frac{1}{2\pi}\int_{-\infty}^{\infty} \mathrm{e}^{\mathrm{i}ht}\, u(\omega, h)\, \mathrm{d}h = \frac{\omega^2\tilde{\gamma}}{[1 + \omega^2\tilde{\gamma}t]^2}, \tag{60}$$

with the constant $\tilde{\gamma} \equiv \alpha_{mm}/\gamma_{\mathrm{h}}$. These results are given in Burridge *et al.* (1989). From the definitions above we find the limiting local (or windowed) power spectral density

$$S_t(\omega) = \int_{-\infty}^{\infty} \mathrm{e}^{\mathrm{i}\omega\sigma}\, C_{t,f}(\sigma)\, \mathrm{d}\sigma = |\hat{f}(\omega)|^2\, \mu(t, \omega), \tag{61}$$

and the corresponding local correlation function

$$C_{t,f}(\sigma) = \frac{1}{2\pi}\int_{-\infty}^{\infty} \mathrm{e}^{-\mathrm{i}\omega\sigma}\, |\hat{f}(\omega)|^2 \frac{\omega^2\tilde{\gamma}}{[1 + \omega^2\tilde{\gamma}t]^2}\, \mathrm{d}\omega. \tag{62}$$

This formula gives the rate of decay in time of the correlation function for the reflected velocity potential. When $\sigma = 0$, (62) gives the mean-square of the reflected velocity potential and if $\hat{f}(0) \neq 0$ and is finite then

$$C_{t,f}(0) = E\{[R_{t,f}(0)]^2\} \sim \frac{\text{constant}}{t^{\frac{3}{2}}} \quad \text{as } t \to \infty. \tag{63}$$

In §10 we give the numerical validation of this theory. We compare $C_{t,f}(0)$, as a function of time t, with the results obtained from a series of numerical experiments.

The theory we have outlined above, based on Burridge *et al.* (1989), works for incident wave pulses that are Gaussian-like in the velocity potential and have therefore N-shaped incident wave elevation, as we noted at the end of §2. The theory can be extended to incident pulses with Gaussian-like wave elevation so that the incident velocity potential is S-shaped. In that case the Fourier transform of the pulse function $f(t)$, $\hat{f}(\omega)$, behaves like ω^{-1} near $\omega = 0$. Formula (62) is still valid even if $|\hat{f}(\omega)|^2 \sim \omega^{-2}$ for ω near zero. However, the long-time behaviour of the reflected wave potential is different to (63):

$$C_{t,f}(0) \sim \frac{\text{constant}}{t^{\frac{1}{2}}} \quad \text{as } t \to \infty. \tag{64}$$

This is the main difference between a Gaussian-like incident wave elevation and an N-shaped one.

8. Calculating the effective parameters for scattering

Through conformal mapping we are able to do scattering for bottom variations of large amplitude. As presented in §3 we decompose the full wave propagation problem into two distinct stochastic problems. First, we have a purely geometrical one in which we transform a random coefficient $n(x)$ into a smoother random coefficient $m(\xi)$. No dynamics is involved. The second problem is the scattering problem presented in §6 with $m(\xi)$ a given stochastic process.

The final result for the scattering problem, namely the reflection statistics, depends on a single number α_{mm} defined at (41). In order to calculate its value we must solve the conformal map problem. Dias & Vanden-Broeck (1989) present the solution for a steady free-surface flow past a submerged triangular obstacle of arbitrary height. Their solution is based on a conformal mapping that has singularities located at the apex and base of the triangle. The fact that they consider the flow to be incompressible, irrotational and steady means that their potential and stream functions are analogous to our variables ξ and ζ. We could then extend their solution to a sequence of triangular obstacles of random height and width or we could use the Schwarz–Christoffel transformation for a polygonal profile. The Schwarz–Christoffel transformation lends itself readily to the numerical calculation of α_{mm} for polygonal bottom topographies.

In the present paper we compute the parameter α_{mm} in a simpler fashion, assuming that the bottom fluctuations are small. From (15) we see that $m(\xi)$ is given as the convolution of a smooth kernel with the composition of the random perturbation and the real part of the conformal map. We have assumed, up to now, that $n(x)$ is an $O(1)$ perturbation. We now assume that in fact $n(x) = \delta N(x)$ and we expand $x(\xi, -\gamma_h; \delta) \equiv x^\delta(\xi, -\gamma_h)$ in terms of the small parameter δ. Start by considering the problem

$$\begin{aligned} &\Delta\xi(x,y) = 0, \\ &\xi_y = 0 \quad \text{at} \quad y = 0, \\ &\xi_n = \xi_y + \delta\gamma_h N'(x)\,\xi_x = 0 \quad \text{at} \quad y = -\gamma_h(1+\delta N(x)). \end{aligned}$$

To solve this problem using perturbation theory we first approximate the equations as follows:

$$\begin{aligned} &\Delta\xi(x,y) = 0, \\ &\xi_y = 0 \quad \text{at} \quad y = 0, \\ &\xi_y + \delta\gamma_h(N'(x)\,\xi_x - N(x)\,\xi_{yy}) + O(\delta^2) = 0 \quad \text{at} \quad y = -\gamma_h. \end{aligned}$$

Assume the solution to be of the form $\xi^\delta(x,y) = \xi_0(x,y) + \delta\xi_1(x,y) + \ldots$. It is clear that ξ_0 should be equal to x. Fourier transforming the order δ equations we find that

$$\xi^\delta(x,y) = x + \delta\xi_1(x,y) + O(\delta^2), \tag{65}$$

with

$$\xi_1(x,y) = \int_{-\infty}^{\infty} \mathrm{i}k\gamma_\mathrm{h} \frac{\cosh ky}{\sinh k\gamma_\mathrm{h}} \hat{N}(k)\, \mathrm{e}^{\mathrm{i}kx}\, \mathrm{d}k. \tag{66}$$

Inverting relation (65) at the undisturbed bottom, we have

$$x^\delta(\xi, \gamma_\mathrm{h}) = \xi + \delta g(\xi) + O(\delta^2) \tag{67}$$

with

$$g(\xi) \equiv \int_{-\infty}^{\infty} \mathrm{i}k\gamma_\mathrm{h} \coth(k\gamma_\mathrm{h}) \hat{N}(k)\, \mathrm{e}^{\mathrm{i}k\xi}\, \mathrm{d}k. \tag{68}$$

The random coefficient in the evolution equation becomes

$$m(\xi) \approx \delta(K*N)(\xi) + \delta^2 (K*N'g)(\xi), \tag{69}$$

where the kernel K is defined in (15). We must now calculate

$$\begin{aligned} \alpha_{mm} &\equiv \frac{1}{2}\int_{-\infty}^{\infty} C_m(s)\, \mathrm{d}s \\ &\approx \delta^2 \left[\alpha_{\tilde{N}\tilde{N}} + \delta \int_0^{\infty} E\{(K*N)(s)\,(K*N'g)(0) + (K*N)(0)\,(K*N'g)(s)\}\, \mathrm{d}s \right]. \end{aligned} \tag{70}$$

We have called $(K*N)(s)$ as $\tilde{N}(s)$. By noting that $2\alpha_{\tilde{N}\tilde{N}} = \hat{C}_{\tilde{N}}(k)|_{k=0}$ it is easy to see that $\hat{C}_{\tilde{N}}(0) = \hat{C}_N(0)$ and therefore $\alpha_{\tilde{N}\tilde{N}} = \alpha_{NN}$. Thus the smoothing effect is not present in the first term. We may write

$$\tilde{\gamma} = \frac{\alpha_{mm}}{\gamma_\mathrm{h}} \approx \frac{\alpha_{nn}}{\gamma_\mathrm{h}} = \delta^2 \frac{\alpha_{NN}}{\gamma_\mathrm{h}}. \tag{71}$$

9. The numerical method

Two numerical methods were tested. A comparison between the finite-difference method and the boundary-element method can be found in Nachbin (1989) and Nachbin & Papanicolaou (1992). The latter uses a boundary integral formulation for Laplace's equation and reproduces very well the dispersive nature of gravity waves. We present a brief description of the method. The boundary $\partial\Omega$ of our computational domain is divided into four parts:

Γ_1 and $\Gamma_4 \rightarrow$ left-hand and right-hand ends of $\partial\Omega$,

$\Gamma_2 \rightarrow$ linear free surface,

$\Gamma_3 \rightarrow$ impermeable random bottom.

The integral formulation for the potential ϕ is essentially the same as the one presented by Salmon, Liu & Liggett (1980). The boundary integral equation (BIE) is provided by Green's third identity:

$$\beta\theta_P \phi(\boldsymbol{P}, t) = \oint_{\partial\Omega} \left(\phi(\boldsymbol{Q}, t) \frac{\mathrm{d}\ln\rho}{\mathrm{d}\bar{n}} - \phi_{\bar{n}}(\boldsymbol{Q}, t) \ln\rho \right) \mathrm{d}\boldsymbol{Q}. \tag{72}$$

In this equation $\phi(\boldsymbol{P})$ denotes symbolically the potential evaluated at a point $\boldsymbol{P}$ along the boundary $\partial\Omega$. The same applies to the point $\boldsymbol{Q}$. In the integral, $\mathrm{d}\boldsymbol{Q}$ designates a

line element. The constant θ_P is equal to π when $\boldsymbol{P}$ is a point at a smooth segment of $\partial\Omega$ and is equal to the internal angle at corners. Details can be found in Brebbia, Telles & Wrobel (1984), Jaswon & Symm (1977) and Nachbin (1989). The boundary conditions are:

$$\text{the radiation condition} \quad \frac{1}{\beta^2}\phi_{\bar{n}} = -\phi_t \quad \text{at} \quad \Gamma_1, \Gamma_4, \tag{73}$$

$$\text{the free surface conditions} \quad \left.\begin{aligned} \phi_t &= -\eta \\ \eta_t &= (1/\beta^2)\phi_y \end{aligned}\right\} \text{ at } \Gamma_2, \tag{74}$$

$$\text{and the bottom condition} \quad \phi_{\bar{n}} = 0 \quad \text{at } \Gamma_3. \tag{75}$$

The water elevation is given by $\eta(x,t)$. These equations are slightly different from those found in Salmon *et al.* (1980) because we have scaled our equations differently (Nachbin 1989; Rosales & Papanicolaou 1983; Whitham 1974). We have introduced the parameter $\beta = h_0/\lambda$, where λ is a typical wavelength. Note that the boundary integral formulation enables the Neumann condition (along Γ_3) to be implemented in a very simple fashion for any random bottom profile. The notation adopted is: $\mathrm{d}/\mathrm{d}\bar{n} = (\beta^2\partial_x, \partial_y)\cdot(n_1, n_2)$, $\boldsymbol{n}$ is the normal vector and $\rho = [(x_p - x_q)^2 + \beta^2(y_p - y_q)^2]^{\frac{1}{2}}$.

The Point Collocation Method (Brebbia *et al.* 1984) is used in the discretization of the BIE, where a linear finite-element approximation is used for the potential and its derivative.

The differencing schemes for the boundary conditions are also given in Salmon *et al.* (1980). The implicit free-surface condition

$$\frac{\phi^{n+1} - \phi^n}{\Delta t} = -\left[\eta^n + \frac{\Delta t}{2\beta^2}(\theta\phi_y^{n+1} + (1-\theta)\phi_y^n)\right] + O(\Delta t^2)$$

is imposed in the discrete BIE, while

$$\frac{\eta^{n+1} - \eta^n}{\Delta t} = \frac{\phi^{n+1} + \phi^n}{2\beta^2} + O(\Delta t^2)$$

is used to update η. The parameter θ is taken to be equal to $\frac{1}{6}$, which leads to a higher-order numerical dispersion relation (Nachbin 1989; Nachbin & Papanicolaou 1992).

10. The numerical experiments and comparison with the theory

10.1. *Introduction*

The rapid variations in the bottom topography prevent a simplification of the water wave equations. The (hyperbolic) shallow-water equations are not valid (Hamilton 1977) and we must use the full linear water wave equations, which are dispersive. The parameter β is taken to be small, but finite ($\beta = 0.08$), and long channels will be considered. The initial data used has a full band of frequencies and therefore numerical dispersion has to be kept at a very low level. Tests verifying the accurate dispersive behaviour of the method were performed and are presented in detail elsewhere (Nachbin 1989; Nachbin & Papanicolaou 1992). The boundary-element method led to very good results.

Channels with rapidly varying periodic bottoms were also tested. As expected, no reflection is observed. Nevertheless the wave has an effective shallow-water speed smaller than one, as predicted in Rosales & Papanicolaou (1983). In contrast, when

we add a small random perturbation to the periodic bottom profile the reflection increases substantially, which is a manifestation of localization. These experiments are shown in Nachbin (1989) and Nachbin & Papanicolaou (1992).

10.2. *The geometry of each problem*

In each realization the underlying flat channel is defined by the rectangle $[-2, 23]\times[-1, 0]$. Along the segment $\{2.0 < x < 22.0;\ y = -1.0\}$ of the bottom we add random $O(1)$ perturbations generated as follows. Consider the random variables h_ω and b_ω to be uniformly distributed in $[-\delta, \delta]$ and $[-0.3l_b,\ 03.l_b]$ respectively. The parameter l_b, as defined earlier, is a typical length of the bottom inhomogeneities. Consider an uniform partition of the interval [2.0, 22.0] into segments of size l_b. Perturb randomly the position of each interior node of this partition by b_ω, the sign indicating to the left $(-)$ or to the right $(+)$. Attach to these positions the random vertical perturbations h_ω to the undisturbed bottom. Connecting these points by straight lines we have the rough bottom's profile. Moreover, the bottom along $x \leqslant 2.0$ and $x \geqslant 22.0$ is flat ($y = -1.0$). At the ends $x = -2.0$ and $x = 23.0$ we impose the radiation condition which allows waves of unit speed to propagate out of the computational domain.

Consider the function

$$\psi(x,t) = 1/(0.5\gamma_p)^{\frac{1}{2}}\exp\left(-(x-t)^2/(0.5\gamma_p)^2\right).$$

The initial conditions, along the free surface, are:

$$\phi(x,0,0) = \psi(x,0), \quad \eta(x,0) = -\frac{\partial}{\partial t}\psi(x,0), \quad \frac{\phi_y(x,0,0)}{\beta^2} = -\frac{\partial^2}{\partial t^2}\psi(x,0).$$

The values of γ_p considered are such that at the ends of the channel the potential is taken to be zero. A typical geometry is given in figure 2.

In order to record the potential for the reflected and the transmitted waves, two fixed points (nodes) are chosen. One is at the beginning of the rough region (node with coordinates $x \approx 2.0$ and $y = 0$) and the other at the end ($x \approx 22.0$ and $y = 0$). The waves used in our experiments will travel over the rough channel (approximately 20 times its length) and will propagate out of the computational domain without reflecting at the end $x = 23.0$ owing to the radiation condition imposed. In the numerical experiments waves propagate from left to right while in the theory we had incoming pulses. from the right. This does not really matter as long as we have reflection being recorded at the beginning of the rough region. The dimensionless shallow-water speed is one and we allow our code to run for about 45 time units so that disturbances generated at the end of the rough region return to the reflection node defined above. Calling this node x_j, we are able to record for each channel sampled (say labelled by ω_n) the reflected signal $R_{x_j}(t;\omega_n) = \phi(x_j, 0, t;\omega_n)$.

10.3. *The theoretical curves*

The theoretical curves are constructed by using (62) and the approximations obtained in §8. We will compute the integral numerically, at the centre $\sigma = 0$ of the window, for each value of t (time).

The parameter $\tilde{\gamma}$ is approximated by $\delta^2\alpha_{NN}/\gamma_h$. In §6 the Fourier transforms took into account the pulse's width. The theoretical curves will have as reference a pulse of unit width. Thus from the definition of the parameter γ_p the following calculations are done with the effective correlation lengths ϵ/γ_p.

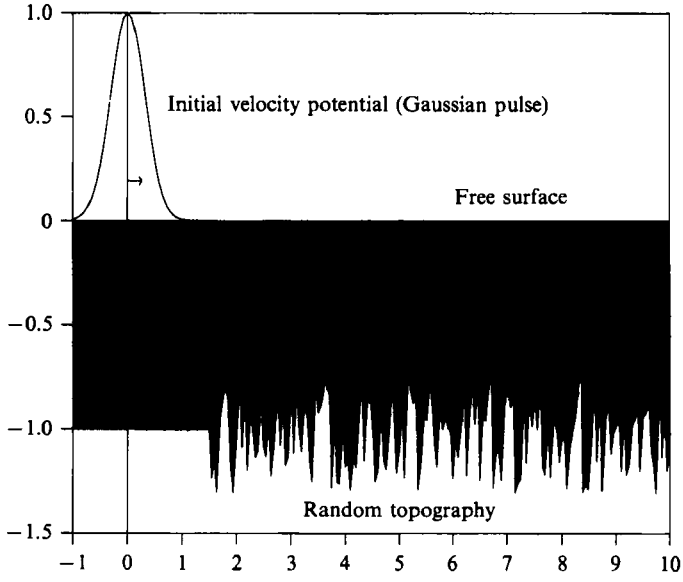

FIGURE 2. A detailed view (of the left-hand end) of a channel with a rapidly varying random topography.

Along each segment of the continuous piecewise-linear bottom profile we write the random perturbation as

$$N(x_i+s;\omega) = \frac{\epsilon/\gamma_p - s}{\epsilon/\gamma_p} N(x_i;\omega) + \frac{s}{\epsilon/\gamma_p} N(x_{i+1};\omega) \quad (s \in [0, \epsilon/\gamma_p]),$$

where s is a local coordinate within this segment. Considering the stochastic process to be stationary it follows that

$$E\{N(s;\omega)N(0;\omega)\} = \begin{cases} (\epsilon/\gamma_p - s)/(\epsilon/\gamma_p)\, E\{N^2(x_i)\} & (0 \leqslant s < \epsilon/\gamma_p). \\ 0 \quad s \geqslant \epsilon/\gamma_p. \end{cases}$$

Assuming that the stochastic process $N(s;\omega)$ is uniformly distributed in $[-\gamma_h, \gamma_h]$ we have that

$$\alpha_{NN} = \int_0^{\epsilon/\gamma_p} E\{N(s)N(0)\}\,ds = \tfrac{1}{6}(\epsilon/\gamma_p)\,\gamma_h^2, \tag{76}$$

$$\tilde{\gamma} \approx \frac{\epsilon\delta^2\gamma_h}{6\gamma_p}. \tag{77}$$

In our experiments $\gamma_h = 1$, $\delta = 0.3$, $l_b = \epsilon = 0.1$ and $\gamma_p = 0.7$, 1.0 and 1.3.

From the initial data, where f denotes the pulse-shaped potential, it is clear that

$$\hat{f}(\omega) = \int_{-\infty}^{\infty} e^{i\omega\tau} f(\tau)\,d\tau = (2\pi)^{\frac{1}{2}} \exp(-\tfrac{1}{2}\omega^2) \quad \text{where } \tau = t/\epsilon.$$

The values of $C_{t,f}(0)$ are computed, as a function of time, using a Gauss–Hermite quadrature (Abramowitz & Stegun 1968) and are shown in figures 3 and 4.

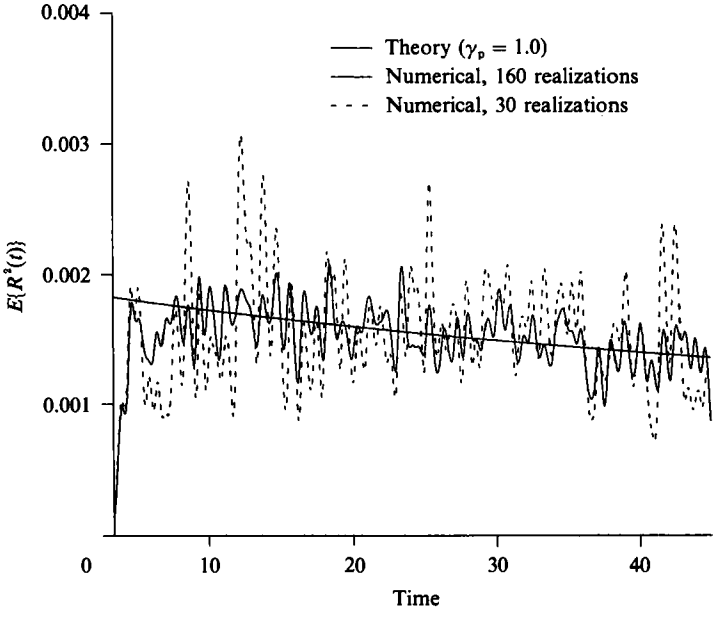

FIGURE 3. Numerical validation of the asymptotic theory and convergence to the limiting function.

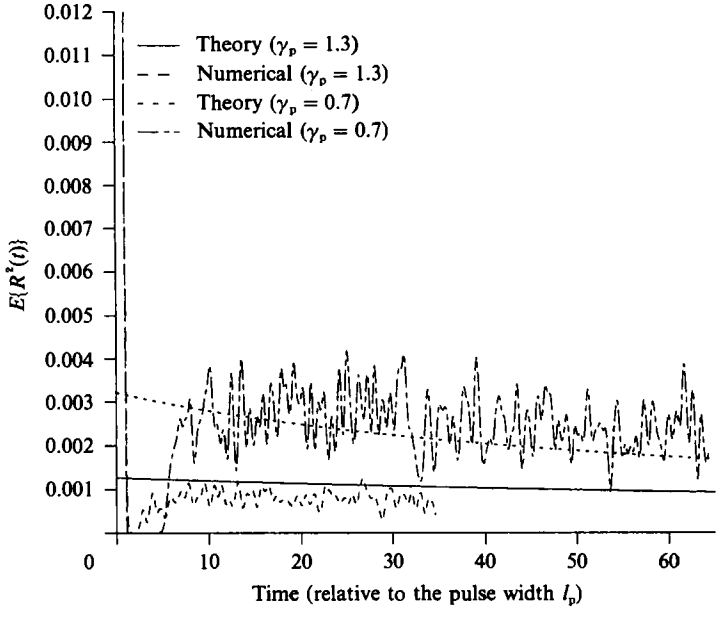

FIGURE 4. Comparison using different correlation lengths.

10.4. *Numerical validation of the theory*

Using the theory presented (§7) we write

$$C_{t,f}(0) = E\{R^2_{x_j}(t)\} \approx \frac{1}{N}\sum_{n=1}^{N} \phi^2(x_j, 0, t; \omega_n),$$

for N large enough (N is the number of realizations). The left-hand side is computed from the theory and the right-hand side from the numerical experiments.

In figure 3 we see that the theoretical and numerical curves are in good agreement. As we take more realizations into account the fluctuations stabilize and converge is evident. In figure 4 we compare different scales. By letting γ_p vary we have wider or thinner pulses and we can see the effect on the results. Thinner pulses will generate more reflection. Their spectra have a broader range of frequencies and localization of the higher modes is felt in the reflected signal. We may say that the pulse sees more details of the bottom topography. The wider pulses tend to average the fluctuations from the bottom's inhomogeneities. The amount of reflection is smaller as well as the amplitude of the fluctuations. We note that for the wider pulse the results are not as accurate as in the other cases. There are two possibilities. One is that we probably need a more accurate value for the parameter $\tilde{\gamma}$, by including more terms from the expansion in δ or by using a Schwarz–Christoffel transformation (cf. §8). The other is to use a more general idea which uses the localization length as a scaling quantity (Sheng *et al.* 1986; White *et al.* 1987).

The discretization of a long channel with a rapidly varying bottom requires a very fine mesh. We used two linear boundary elements along each side Γ_1 and Γ_4, 636 along the free surface Γ_2 and 680 at the bottom Γ_3. Thus we have two dense non-symmetric matrices (of order 1320) to be calculated. For the evolution scheme a total of 2700 timesteps (for the 45 time units) are considered. A supercomputer is used and vectorization plays an important role. Each realization takes less than 2 min of CPU time. To compute the results for 160 different channels (cf. figure 3) it takes approximately 5 h on an ETA10.

11. Conclusions

We have considered water-wave propagation in shallow channels with rapidly varying random topography. The scaling adopted for the linear water-wave equations emphasizes a geometry in which the typical depth is comparable to the horizontal and vertical lengths of the bottom's irregularities. Hence, order one perturbations are considered. This scaling prevents an asymptotic simplification at the level of the equations. The full linear potential theory must be used.

We presented an asymptotic theory for the statistics of the reflected signal. The derivation of a system of stochastic differential equations for the amplitudes of the propagating and evanescent modes is most convenient when we change variables and transform our channel to a flat one. The interplay between these modes is better understood when we consider monochromatic waves (time harmonic case).

The application of an asymptotic theory for the solution of the stochastic differential equations allow us to characterize the expected value of the transmission coefficient. For an incident monochromatic wavetrain of unit amplitude and frequency ω we have (we repeat our results for convenience):

$$E\{|T|^2\} \sim \exp\left(-\frac{\gamma_L \omega^2}{8\gamma_h^2}\alpha_{mm}\right)\int_{-\infty}^{\infty}\exp\left(-t^2\frac{\gamma_L\omega^2}{2\gamma_h^2}\alpha_{mm}\right)\frac{\pi t\sinh\pi t}{\cosh^2\pi t}\,\mathrm{d}t.$$

On a practical application, where we can ignore other dissipative mechanisms such as viscosity (see Devillard *et al.* 1988 for a discussion on this matter), the formula above can be used to estimate how much transmission is obtained at the end of the rough region of the channel. If the relative scales are the same as in this paper, all we need to do is to define the values of the parameters $\gamma_L = L/h_0$ and $\gamma_h = h_0/l_b$ (which depend on the typical lengths of the channel) and compute the value of the

parameter α_{mm} by integrating the correlation function of the random perturbation (cf. (41)). We give an example of how to compute α_{mm} in §10.3. The expected value for the transmission coefficient follows by computing the integral above.

The time-harmonic case shows that the theory developed leads to results that are basically the same as for the acoustic wave equation (for which we could make an analogy with the shallow-water equations). An extensive set of references for the acoustic theory is given in the review paper by Asch *et al.* (1991). For the propagation of a pulse we use the results obtained for acoustic pulse waves (see Burridge *et al.* 1989). We considered the initial water-wave potential to be a Gaussian pulse which is long compared to the bottom variations and which propagates over long distances. The expected value for the reflection coefficient is obtained by evaluating the correlation function (of the reflection process) at the centre $\sigma = 0$ of the windowed process (cf. (62)):

$$C_{t,f}(0) = \frac{1}{2\pi}\int_{-\infty}^{\infty} |\hat{f}(\omega)|^2 \frac{\gamma_h \omega^2 \alpha_{mm}}{[\gamma_h + \omega^2 \alpha_{mm} t]^2} \mathrm{d}\omega.$$

This result shows the finite depth effect through the parameter γ_h. We again point out that only the correlation function of the random $O(1)$ depth perturbation plays a role in the final result, through the parameter α_{mm}. Given that the initial pulse shape f is known (and consequently its Fourier transform $\hat{f}$) we can readily estimate the decay of the correlation function of the reflection process by numerical integration of the expression above. We graphed time-dependent curves for $C_{t,f}(0)$ and we compared them with the statistical properties of our numerical experiments.

The boundary-element method approximates very well the dispersive nature of gravity waves and is therefore the preferred numerical method for our study of reflection and transmission of long waves in a shallow channel with irregular bottom topography. We generated continuous piecewise-linear random bottom profiles using a random-number generator. For each realization of the bottom topography we allowed a Gaussian pulse (for the potential) to propagate over the rough region and we recorded the reflected signal. We then computed the statistical properties of the numerical reflected signals. We have found good agreement between the theory and numerical computations. Thus not only have we validated our asymptotic theory numerically but also we have shown that the boundary-element method is a reliable and efficient tool for application problems in linear water-wave propagation.

A. Nachbin's work has been supported by the Brazilian Ministry of Education (CAPES) and by the National Science Foundation under grant DMS 9003227.

REFERENCES

ABRAMOWITZ, M. & STEGUN, I. A. 1968 *Handbook of Mathematical Functions*. Dover.

ARNOLD, L., PAPANICOLAOU, G. & WIHSTUTZ, V. 1986 Asymptotic analysis of the Lyapounov exponent and rotation number of the random oscillator and applications. *SIAM J. Appl. Maths* **46**, 427–450.

ASCH, M., KOHLER, W., PAPANICOLAOU, G., POSTEL, M. & WHITE, B. 1991 Frequency content of randomly scattered signals. *SIAM Rev.* **33**, 519–625.

BELZONS, M., GUAZZELLI, E. & PARODI, O. 1988 Gravity waves on a rough bottom: experimental evidence of one-dimensional localization. *J. Fluid Mech.* **186**, 539–558.

BREBBIA, C. A., TELLES, J. C. F. & WROBEL, L. C. 1984 *Boundary Element Technique*. Springer.

BURRIDGE, R., PAPANICOLAOU, G. C., SHENG, P. & WHITE, B. 1989 Probing a random medium with a pulse. *SIAM J. Appl. Maths* **49**, 582–607.

CARRIER, G. F. 1966 Gravity waves on water of variable depth. *J. Fluid Mech.* **24**, 641–659.

DEVILLARD, P., DUNLOP, F. & SOUILLARD, B. 1988 Localization of gravity waves on a channel with a random bottom. *J. Fluid Mech.* **186**, 521–538.

DIAS, F. & VANDEN-BROECK, J.-M. 1989 Open channel flows with submerged obstructions. *J. Fluid Mech.* **206**, 155–170.

HAMILTON, J. 1977 Differential equations for long-period gravity waves on a fluid of rapidly varying depth. *J. Fluid Mech.* **83**, 289–310.

JASWON, M. A. & SYMM, G. T. 1977 *Integral Equation Methods in Potential Theory and Elastostatics.* Academic.

KELLER, J. B. 1958 Surface waves on water on non-uniform depth. *J. Fluid Mech.* **4**, 607–614.

KOHLER, W. 1977 Power reflection at the input of a randomly perturbed rectangular waveguide. *SIAM J. Appl. Maths* **32** (3), 521–533.

KOHLER, W. & PAPANICOLAOU, G. C. 1973 Power statistics for waves in one dimension and comparison with radiative transport theory I. *J. Math. Phys.* **14**, 1733–1745.

KOHLER, W. & PAPANICOLAOU, G. C. 1974 Power statistics for waves in one dimension and comparison with radiative transport theory II. *J. Math. Phys.* **15**, 2186–2197.

KREISEL, G. 1949 Surface waves. *Q. Appl. Maths* **7**, 21–44.

MEI, C. C. 1983 *The Applied Dynamics of Ocean Surface Waves.* John Wiley.

MEI, C. C. & BLACK, J. L. 1969 Scattering of surface waves by rectangular obstacles in waters of finite depth. *J. Fluid Mech.* **38**, 499–511.

NACHBIN, A. 1989 Reflection and transmission of water waves in shallow channels with rough bottoms. PhD thesis, New York University.

NACHBIN, A. & PAPANICOLAOU, G. C. 1992 Boundary element method for the long-time water wave propagation over rapidly varying bottom topography. *Intl J. Numer. Meth. Fluids* (to appear).

PAPANICOLAOU, G. C. 1978 Asymptotic analysis of stochastic equations. In *Studies in Probability* (ed. M. Rosenblatt), pp. 111–179. MAA Studies in Mathematics, vol. 18.

PAPANICOLAOU, G. C. & KOHLER, W. 1975 Asymptotic analysis of deterministic and stochastic equations with rapidly varying components. *Commun. Math. Phys.* **45**, 217–232.

ROSALES, R. R. & PAPANICOLAOU, G. C. 1983 Gravity waves in a channel with a rough bottom. *Stud. Appl. Maths* **68**, 89–102.

SALMON, J. R., LIU, P. L.-F. & LIGGETT, J. A. 1980 Integral equation method for linear water waves. *J. Hydraul. Div. ASCE* **106** (HY12), 1995–2010.

SHENG, P., ZANG, Z.-Q., WHITE, B. & PAPANICOLAOU, G. 1986 Multiple-scattering noise in one dimension: universality through localization-length scaling. *Phys. Rev. Lett.* **57**, 1000–1003.

WHITE, B., SHENG, P. S., ZANG, Z.-Q. & PAPANICOLAOU, G. 1987 Wave localization characteristics in the time domain. *Phys. Rev. Lett.* **59**, 1918–1921.

WHITHAM, G. B. 1974 *Linear and Nonlinear Waves.* John Wiley.